Electronic Supplementary Information

Hydrogen-Bond Disruption in Molecularly Engineered Janus Evaporators for Enhanced Solar Desalination

Jie Zhu[†a], Dong Wu[†a], Xiayun Huang[*a], Daoyong Chen[a, b], Zhihong Nie[*a]

[a] The State Key Laboratory of Molecular Engineering of Polymers and Department of Macromolecular Science, Fudan University, Shanghai, 200438, People's Republic of China

[b] The Key Laboratory of Functional Molecular Solids, Ministry of Education, and Department of Materials Chemistry, School of Chemistry and Materials Science, Anhui Normal University, Wuhu, Anhui, 214002, People's Republic of China

†Equal contributions.

Corresponding Author: huangxiayun@fudan.edu.cn (X. Huang); znie@fudan.edu.cn (Z. Nie)

This PDF file includes:

Supplementary Text

Note S1 Estimation of the evaporation efficiency

The evaporation efficiency (η, %) of Q1-30, Q1-60 and Q1-90 was calculated by the **Equation S1**,

$$\eta = \frac{r \times E_{equ}}{q_{solar}} \qquad \textbf{(Equation S1)}$$

where r was the evaporation rate (kg m^{-2} h^{-1}) after reaching the steady evaporation state, E_{equ} was the equivalent enthalpy (J g^{-1}) obtained by the dark experiment, q_{solar} was the solar flux (kW m^{-2}).[1] The initial ambient temperature and the humidity of the surroundings in the dark experiment were fixed at 25 °C and 45%, respectively. In the dark experiment, the E_{equ} can be estimated by vaporizing water with identical power input, which has the relationship shown in the **Equation S2**,

$$E_0 \times M = E_{equ} \qquad \textbf{(Equation S2)}$$

where E_0 is the evaporation enthalpy (J g^{-1}) of water and M is the ratio of mass change of bulk water over evaporators. Based on the above equations, the measured equivalent enthalpy and calculated efficiency of water were 2390 J g^{-1} and 21%, which were very close to the reference values (2450 J g^{-1} and 20%),[2] confirming the accuracy of our measurements and calculations.

Note S2 Molecular dynamics (MD) simulations

All molecular dynamics (MD) simulations were conducted using the 'condensed-phase optimized molecular potentials for atomistic simulation studies (COMPASS)' force field within the Materials Studio software (Accelrys Inc.).[3-5] To calculate the average number of hydrogen bonds per water molecule and the diffusion coefficient of water molecules, each MD model consisted of either 1000 water molecules alone or 6 polymer chains and 1000 water molecules, with the cubic box length adjusted to match the experimental density and exceed twice the van der Waals radius.

Simulations began with a relaxed system under periodic boundary conditions, and structural optimizations were conducted using the Smart algorithm. Following energy minimization, the configuration with the lowest total energy was pre-equilibrated in the NPT ensemble at 298 K for 100 ps using the Berendsen method. Periodic boundary conditions were applied in all three dimensions. The production run was performed in the NVT ensemble at 298 K with a time step of 1 fs using a Nose thermostat. Long-range electrostatic interactions were computed using the Ewald method with a relative tolerance of 1×10^{-6}, while a cutoff distance of 12.5 Å was applied for both real-space Ewald and van der Waals interactions. After 1000 ps of MD simulation, hydrogen bonds were analyzed using built-in tools.[6] Trajectory data were saved every 10 ps to calculate the mean square displacement (MSD) of water molecules over time.[7, 8] The MSD, proportional to the observation time at its limit, was used to calculate the diffusion coefficient of water molecules (D), based on the following equation:

$$D = \frac{1}{2d}\lim_{t\to\infty}\frac{\langle|r(t)-r(0)|^2\rangle}{t} \qquad \textbf{(Equation S3)}$$

where r represents the position of the center of mass of a water molecule, and d is the dimensionality of the system (d = 3 for three-dimensional simulations). In **Equation S3**, the numerator represents the MSD.

For interaction energy (E_{int}) calculations, the system comprised either 2 water molecules alone or 1 polymer chain and 10 water molecules, with geometry optimization performed using the same method as described above.[9, 10] E_{int}, representing the interaction strength between system components, was calculated using the following equation, where more negative values indicate stronger interactions:

$$E_{int} = E_{total} - \sum E_{component} \quad \textbf{(Equation S4)}$$

where E_{total} represents the total energy of the system, and $E_{\text{component}}$ represents the energy of each component in the system.

Supplementary Figures

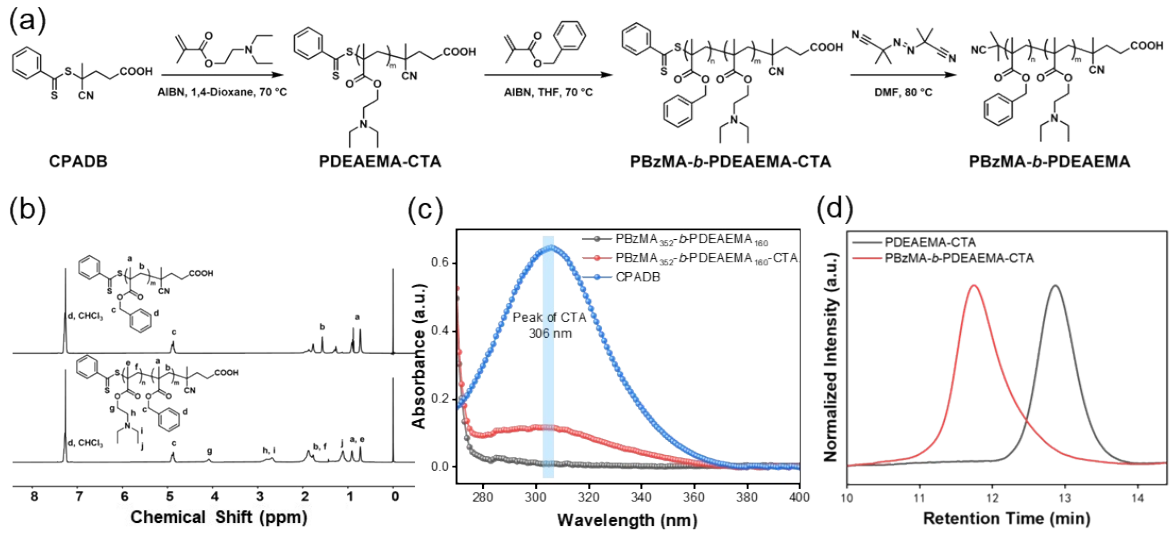

Fig. S1 (a) Synthetic routes for PBzMA-*b*-PDEAEMA. (b) ^{1}H NMR spectra of $PBzMA_{352}$-CTA and $PBzMA_{352}$-*b*-$PDEAEMA_{160}$-CTA. (c) UV-Vis absorbance spectra of CPADB and PBzMA-*b*-PDEAEMA before and after end group modification. (d) GPC traces of PDEAEMA-CTA and PBzMA-*b*-PDEAEMA-CTA.

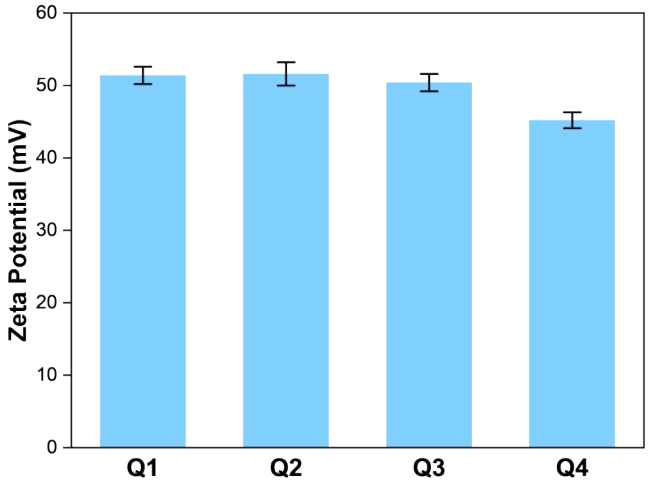

Fig. S2 Zeta potentials of Q1, Q2, Q3 and Q4 micelles.

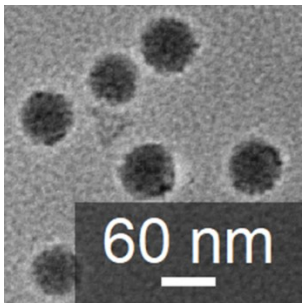

Fig. S3 The magnified TEM image of BE-MeI micelles.

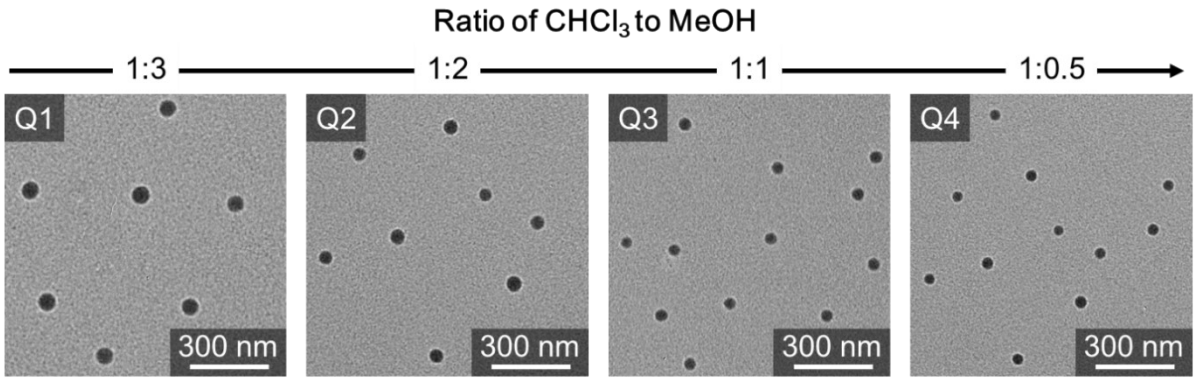

Fig. S4 TEM images of micelles with different solvent ratios.

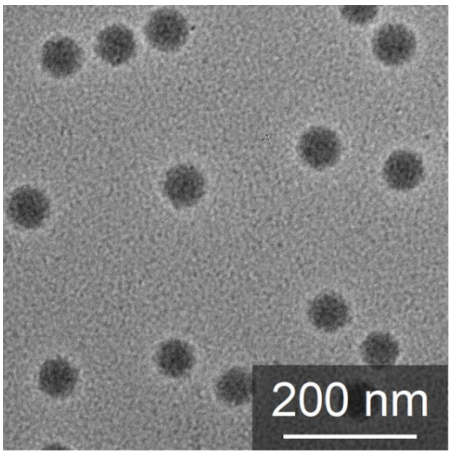

Fig. S5 TEM image of BE-MeI micelles prepared by volume ratio of MeOH/$CHCl_3$ at 4:1. Resultant micelle core size (64 ± 2 nm) was similar to that of Q1 (64 ± 3 nm, prepared with volume ratio of MeOH/$CHCl_3$ of 3:1).

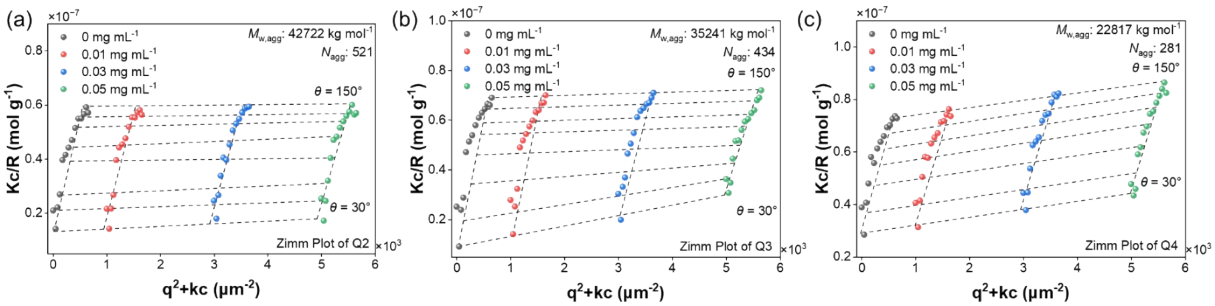

Fig. S6 Zimm plots of (a) Q2, (b) Q3 and (c) Q4 micelles in water.

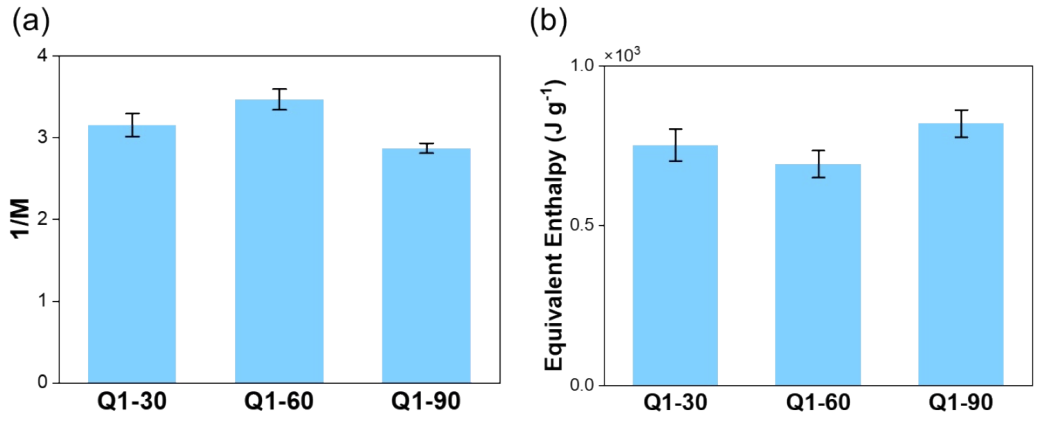

Fig. S7 (a) Water evaporation rate ratio in dark condition and (b) the calculated equivalent enthalpy of Q1-30, Q1-60 and Q1-90.

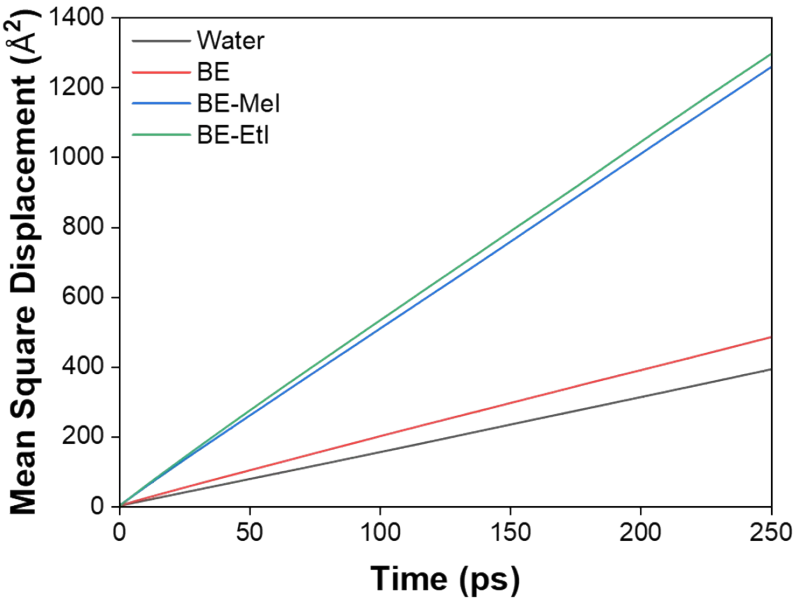

Fig. S8 Mean square displacement of water, BE, BE-MeI and BE-EtI over time.

References

1. Y. Guo, X. Zhao, F. Zhao, Z. Jiao, X. Zhou and G. Yu, *Energy Environ. Sci.*, 2020, **13**, 2087-2095.

2. L. Wu, Z. Dong, Z. Cai, T. Ganapathy, N. X. Fang, C. Li, C. Yu, Y. Zhang and Y. Song, *Nat. Commun.*, 2020, **11**, 521.

3. H. Sun, *J. Phys. Chem. B*, 1998, **102**, 7338-7364.

4. H. Lv, Y. Song, H. Zhang, Y. He, X. Hou, J. Sun and X. Wang, *J. Mol. Liq.*, 2024, **401**, 124750.

5. S. P. Kadaoluwa Pathirannahalage, N. Meftahi, A. Elbourne, A. C. G. Weiss, C. F. McConville, A. Padua, D. A. Winkler, M. Costa Gomes, T. L. Greaves, T. C. Le, Q. A. Besford and A. J. Christofferson, *J. Chem. Inf. Model.*, 2021, **61**, 4521-4536.

6. J. Zhu, X. Zhao, N. Wu, D. Wu, X. Huang, Z. Nie and D. Chen, *Macromolecules*, 2024, **57**, 9811-9822.

7. A. Ghaffari and A. Rahbar-Kelishami, *J. Mol. Liq.*, 2013, **187**, 238-245.

8. S. A. Khrapak, *J. Phys. Chem. B*, 2024, **128**, 287-290.

9. H. Yu, H. Jin, M. Qiu, Y. Liang, P. Sun, C. Cheng, P. Wu, Y. Wang, X. Wu, D. Chu, M. Zheng, T. Qiu, Y. Lu, B. Zhang, W. Mai, X. Yang, G. Owens and H. Xu, *Adv. Mater.*, 2024, 2414045, DOI: https://doi.org/10.1002/adma.202414045

10. L. Han, K. Liu, M. Wang, K. Wang, L. Fang, H. Chen, J. Zhou and X. Lu, *Adv. Funct. Mater.*, 2018, **28**, 1704195.